*Mária Macáková**

Simple Changes of an Object Studied by Holographic Interferometry

Part I

General translations of an object are investigated by double exposition holographic interferometry. A rigorous formula describing the fringe geometry is derived. A method for the determination of all three translation components from the single interference pattern is proposed. The theoretical predictions are verified in a number of experiments.

1. Introduction

By means of the holographic interferometry diffusely reflecting objects and their complex changes can be investigated. In this paper we have studied the possibilities and range of application of double exposition holographic interferometry for general translations of an object. The rotations, where the localization conditions must be treated carefully, are the subject of the next paper.

2. Object Translations

Let us consider the parallel translation of an object between two exposures of a hologram. The translation vector $\boldsymbol{L}$ is the same for each point of the object. After the reconstruction, two waves are obtained belonging to initial and final position of the object respectively. The phase difference between two waves is

$$\Phi = \frac{2\pi}{\lambda}(\boldsymbol{n}_2 - \boldsymbol{n}_1)\cdot\boldsymbol{L}, \tag{1}$$

where $\boldsymbol{n}_1$, $\boldsymbol{n}_2$ are unit vectors along the incident and the scattered rays, respectively, and λ is the wavelength. These two waves interfere and form stationary interference fringes in such a region of space where the phase difference Φ is constant. We shall assume that the object is illuminated by a plane wave ($\boldsymbol{n}_1 =$ = const.) and the reconstruction, is carried out in such a way that the magnifying factor is equal to unity. In this case it is known that for object translations stationary interference fringes at infinity [1] can be observed in which case $\boldsymbol{n}_2$ is nearly constant. Therefore the interference fringes must be observed through a focusing optical system.

Let us introduce a Cartesian coordinate system ξ, η, ζ in the focal plane of an optical observing system. The origin of the reference system is defined as the intersection point of the line of sight with the focal plane (see Fig. 1). The ζ axis is parallel to the line of sight whereas ξ and η lie in the focal plane. The ξ axis

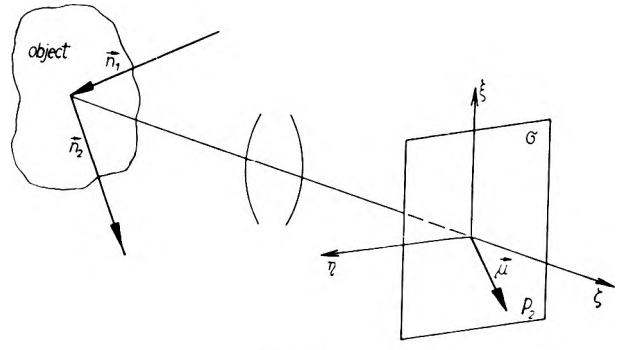

Fig. 1.

is perpendicular to the ζ axis and to the $\boldsymbol{n}_1$ vector. Then the unit vectors ξ_0, η_0, ζ_0 form a righthand rectangular system.

The incident light is scattered in various directions by all the points of the diffuse object. The waves propagating in the $\boldsymbol{n}_2$ direction are then focused through the optical system at the point $P_2(\mu)$ in the focal plane (see Fig. 1.). Thus the position of $P_2(\mu)$ depends on $\boldsymbol{n}_2$. In other words, μ is a function of $\boldsymbol{n}_2$. To analyse, in more detail, the interference picture we need to know the exact form of this function. From Fig. 2 it is clear that μ is parallel to the vector

$$\boldsymbol{n}_2 - \zeta_0 \cos\vartheta,$$

where ϑ is the angle between $\boldsymbol{n}_2$ and the line of sight (ζ_0). Moreover, we know that,

*) Faculty of Engineering, Slovak Technical University, Bratislava, Gottwaldovo nám. 50, Czechoslovakia.

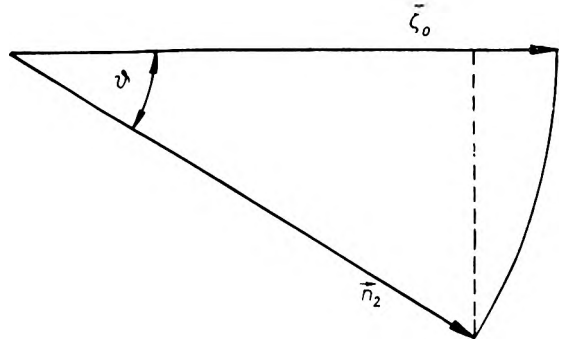

Fig. 2.

$$|\boldsymbol{\mu}| = f \operatorname{tg} \vartheta, \tag{2}$$

where f is the focal length. Hence it follows that,

$$\boldsymbol{\mu} = \frac{f}{\cos\vartheta}(\boldsymbol{n}_2 - \zeta_0 \cos\vartheta) \tag{3}$$

and conversely

$$\boldsymbol{n}_2 = \frac{\zeta_0 + \dfrac{\boldsymbol{\mu}}{f}}{\sqrt{1+\left(\dfrac{\boldsymbol{\mu}}{f}\right)^2}}. \tag{4}$$

Denoting $\dfrac{\boldsymbol{\mu}}{f} = \boldsymbol{\tau}$, $\boldsymbol{n}_1 \cdot \boldsymbol{L} = L_1$ and substituting eq. (4) into eq. (1) we get for the phase difference

$$\Phi = \left(L_1 + \frac{\boldsymbol{\tau} + \zeta}{\sqrt{1+\tau^2}} \cdot \boldsymbol{L}\right)\frac{2\pi}{\lambda}. \tag{5}$$

We can see that the fringe geometry depends on the form of the function Φ only. An interference maximum occurs, if $\Phi = 2\pi m$, where m is an integer. Then

$$m\lambda = L_1 - \frac{\boldsymbol{\tau} + \zeta_0}{\sqrt{1+\tau^2}} \cdot \boldsymbol{L}. \tag{6}$$

If we take into account that

$$\boldsymbol{\tau} = \xi\xi_0 + \eta\eta_0$$

and

$$\boldsymbol{L} = L_\xi \xi_0 + L_\eta \eta_0 + L_\zeta \zeta_0$$

eq. (6) becomes

$$\xi L_\xi + \eta L_\eta + L_\zeta = Q\sqrt{1+\xi^2+\eta^2}, \tag{7}$$

where Q denotes $L_1 - m\lambda = m\lambda'$. Thus equation (7) determines the shape of the interference fringes and it appears to be fundamental for our considerations. However, we cannot obtain the interference order Q from the interference pattern, only. Therefore, we must first find the direction of $\boldsymbol{L}$ by an analysis of the shape of the interference fringes. Secondly we can obtain the absolute value of $\boldsymbol{L}$ from the fringe spacing.

Let us consider any interference fringe and choose three points $P_i(\xi_i, \eta_i, 0)$, $(i = 1, 2, 3)$ on it. When we substitute their coordinates (after normalizing by f, $\boldsymbol{\tau} = \dfrac{\boldsymbol{\mu}}{f}$) into eq. (7) and divide it by the factor $Q = Q_1 = Q_2 = Q_3$, we obtain

$$\xi_i L'_\xi + \eta_i L'_\eta + L_\zeta = \sqrt{1+\xi_i^2+\eta_i^2} \quad (i = 1, 2, 3) \tag{8}$$

where $\boldsymbol{L}' = \dfrac{\boldsymbol{L}}{Q}$. By solving system (8) we obtain $\boldsymbol{L}'$. However $\boldsymbol{L}'$ is parallel to $\boldsymbol{L}$. If we express $\boldsymbol{L}'$ in the spherical coordinates (L', Θ, Ψ) we then have two components of $\boldsymbol{L}(L, \Theta, \Psi)$. The absolute value of $\boldsymbol{L}$ may be found in the following way.

In the interference pattern we choose two fringes with two points P_4, P_5, respectively, in such a way that the interference order is changed monotonically between them. For these points it holds

$$Q_4 = m'_4\lambda,$$
$$Q_5 = m'_5\lambda.$$

Writing eq. (7) for these points and dividing them by the factors $a_i = \sqrt{1+\xi_i^2+\eta_i^2}$ $(i = 4, 5)$ and subtracting each one from the other, we finally obtain

$$L = \frac{p\lambda}{\left|\left(\dfrac{\xi_4}{a_4} - \dfrac{\xi_5}{a_5}\right)\sin\Theta\cos\Psi + \left(\dfrac{\eta_4}{a_4} - \dfrac{\eta_5}{a_5}\right)\sin\Theta\sin\Psi + \left(\dfrac{1}{a_4} - \dfrac{1}{a_5}\right)\cos\Theta\right|}. \tag{9}$$

Here $p = |m_4 - m_5|$ is the number of the fringes between P_4 and P_5, which includes one or the other of them.

However, we must remember that the sign of $\boldsymbol{L}$ is ambiguous, because the initial and final object position are interchangeable.

5. Experimental Results

A diagram of the experimental setup is shown in Fig. 3. The light from the He-Ne laser, with maximum power about 5 mW, passes through the shutter Z and the beam splitter M_1. The reference and object beams are expanded by microscope lenses O_1, O_3 and collimated by lenses O_2, O_4. The object O (an aluminium plate $21 \times 31 \times 14$ mm^3) is placed on the, Zeiss comparator, which allows its movement in the horizontal plane. The distance between the object and the hologram is about 25 cm. During reconstruction the hologram is illuminated with the object

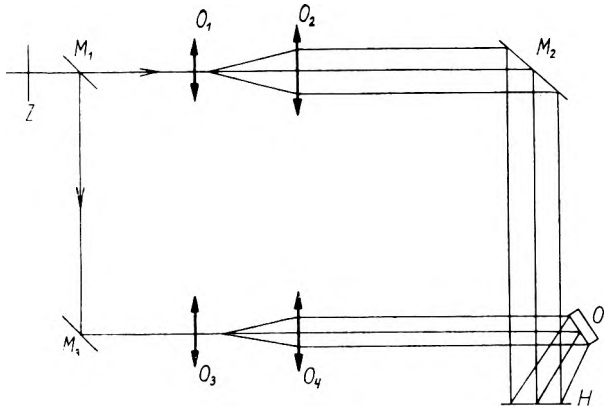

Fig. 3. Diagram of the experimental setup: Z — shutter, M_1 — beam splitter, M_2, M_3 — mirrors, O_1, O_3 — microscope lenses, O_2, O_4 — lenses, O — object, H — hologram

beam to obtain a higher intensity in the reconstructed images.

The accuracy of the method was verified in the case of translations perpendicular to the line of sight. The displacements $(0, L_\eta, 0)$ ranged from 10 up to 500 μm. Fringe spacings were measured from the interference patterns obtained. The calculations were based on eq. (9) where, setting

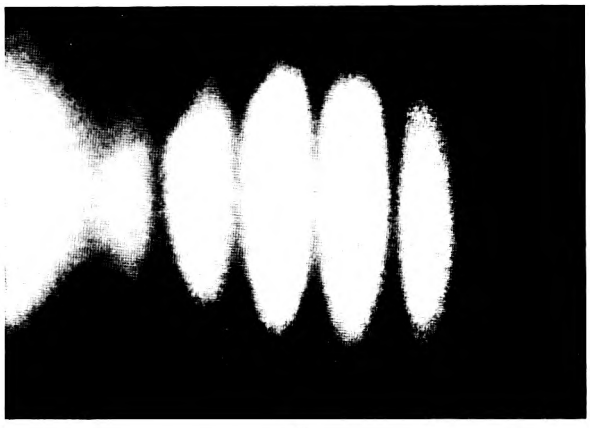

a

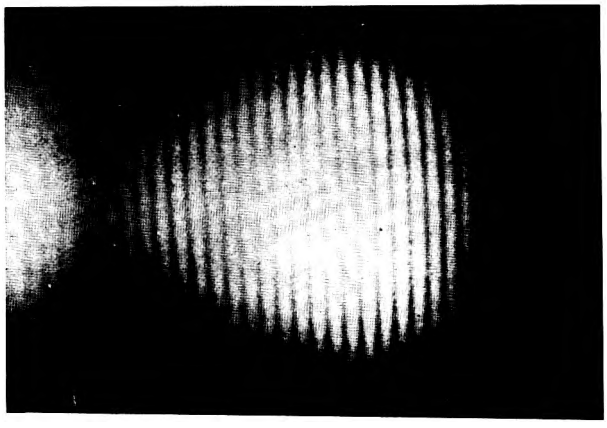

b

Fig. 4. Interference fringes produced from a double-exposure hologram for lateral translations a — $L_\eta = 20$ μm, b — $L_\eta = 90$ μm

$$\Theta = \Psi = \frac{\pi}{2} \text{ and } \alpha_4 = \alpha_5 \cong 1,$$

we found

$$L_\eta = \frac{\lambda p}{\eta_4 - \eta_5}. \tag{10}$$

Here $|\eta_4 - \eta_5|$ means the fringe spacing. The calculated and actual values are compared in Tab. 1. Fig. 4a, b shows the interference patterns for object translations $L_\eta = 20$ μm and $L_\eta = 90$ μm, respectively.

If displacement $\boldsymbol{L}$ are parallel to the line of sight we find that the measurable range becomes larger. This is the case corresponding to the Haindinger fringes in classical interferometry. In our experimental conditions we could study these translations in the range from 250 to 2000 μm. Calculations were based on eq. (9). Fig. 5 shows the interference pattern for $L_\xi = 800$ μm. The calculated and actual values are compared in Tab. 2.

Table 1

L_η meas. [μm]	L_η calc. [μm]	Error [%]
10	10.28	2.8
20	20	0
30	28.6	4.6
40	39	−2.5
49	46.7	−4.7
60.7	61.6	+1.5
70	68.4	−2
80	82	2.5
90	90.6	0.6
100	97	−3
130	131	0.7
160	159.7	0
190	195	2.7
220	215	−2.5
250	262	4.8
275	277	1
310	299	−3
321	316.7	−1.5
330	322	−2.8
373	377.8	1
400	396	−1
450	436	−3
500	518	3.5

Also, we carried out experiments for $\boldsymbol{L}$ with $\Theta = 15°, 30°, 45°, 60°, 75°$. Fringes are curved for $\Theta \leqslant 30°$, only. For $\Theta > 30°$ the fringes are straight lines.

In Tab. 3 there are experimental results for $\Theta = 15°$ and $\Theta = 30°$. Figure 6 shows the interference pattern for $L = 400$ μm, $\Theta = 30°$.

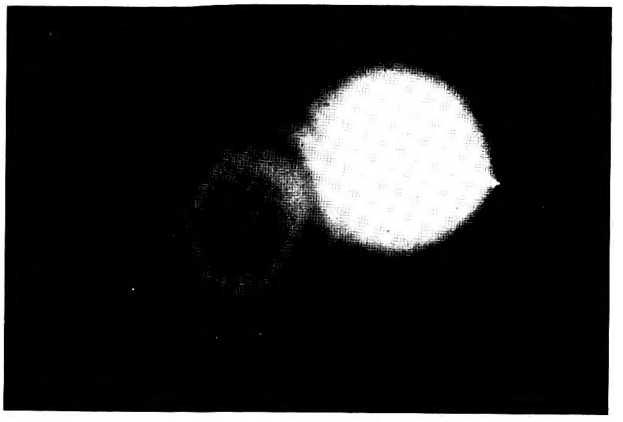

Fig. 5. Example of the interference pattern for a translation along the line of sight $L_\zeta = 800\ \mu m$

It can be seen from our experiments that for $\Theta > 30°$ the information about one component of $\boldsymbol{L}$ can be obtained from the single interference pattern.

Table 2

L_ζ meas. [μm]	L_ζ calc. [μm]	Error [%]
247	224	9.2
400	365	9
484	483	0
500	520	4
600	632	5
700	750	7
800	810	1.5
900	855	5
1000	1014	1.4
1100	1082	2
1200	1113	7
2000	1940	3

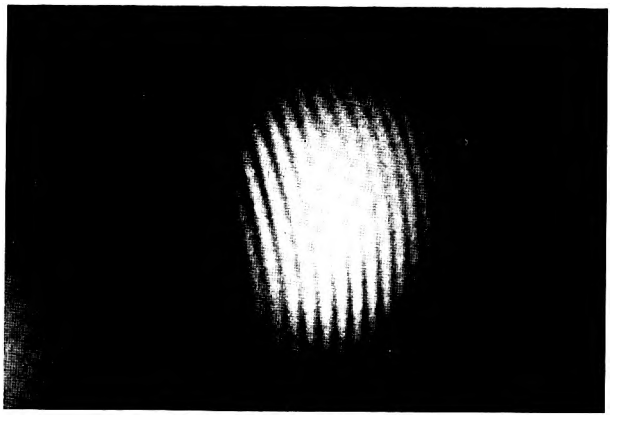

Fig. 6. Illustration of the translation $L = 400\ \mu m$, $\Theta = 15°$

Further it can be shown that the fringe spacing depends considerably on the angle Θ. The fringe spacing vs. Θ for $L = 400\ \mu m$ is plotted in Fig. 7.

Table 3

$\Theta = 15°$

L meas. [μm]	L calc. [μm]	Θ calc.
400	380	15°35′
500	456	15°30′
600	563	11°
800	745	10°
1000	1126	9°

$\Theta = 30°$

L meas. [μm]	L calc. [μm]	Θ calc.
300	335	29°
400	459.5	26°
500	502	30°
600	596	33°
800	732	34°

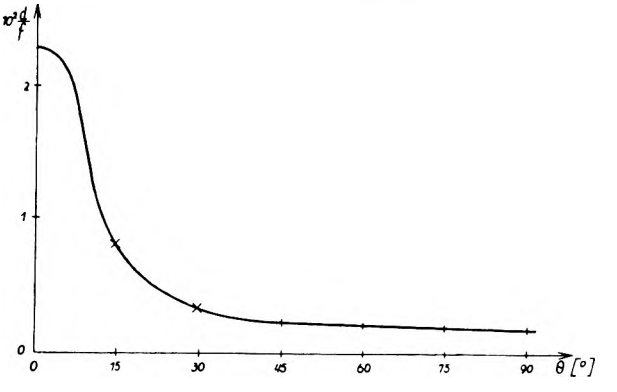

Fig. 7. Dependence of the angle Θ on the fringe spacing d when $L = 400\ \mu m$

4. Conclusion and Discussion

The translations of the object perpendicular to the line of sight have been verified in the range from 10 to 500 μm. The lower limit arises from the necessity to have at least two fringes in the observation area. If the object were larger the limit could be expected to be smaller. The accuracy of the achieved results (about 1-4%) can not be looked at from the standpoint of classical interferometry. The fringes are localized at infinity and the translation vector is calculated from the fringe density in unit angle. The exact measurement of the fringe density or their spacing is limited because of their cosine profile. The fringe position can be measured at best to within an accuracy of 10 % i. e. to within 0.1 of a fringe spacing. If we take into account more than two fringes we

could specify the resulting vector $\boldsymbol{L}$ with a better relative accuracy. But this situation takes place when translations are large, so that the absolute accuracy of the measurements is unchanged, although it can be seen that an accuracy of 1 % may be achieved. Such measurements were also carried out with the same accuracy by FROEHLY *et al.* [2] but only in the range from 10 to 80 μm.

Translations parallel to the line of sight were briefly studied by FROEHLY *et al.* [2] and TSUJIUCHI *et al.* [3]. However Froehly *et al.* did not calculate the translation vector from the interference pattern. Tsujiuchi *et al.* have presented an interference pattern without comparing the experimental and calculated values. Moreover, they introduced the formula for the Haindinger fringes and stated that the translation vector can be calculated from this formula.

However, if we use special illumination ($\boldsymbol{n}_1 =$ = const.), which is necessary for high fringe contrast, there is a great discrepancy between the classical and holographical interference pattern. In holographic interferometry the primary phase difference $\boldsymbol{n}_1 \cdot \boldsymbol{L}$ is constant for all scattered rays and also for fringes. Then identical interference patterns correspond to $\boldsymbol{L}$ twice as large.

In our work we have paid a special attention to the L_ζ translations and to the translations in a general direction. We have studied them in the wide range from 250 to 2000 μm. The accuracy ranging between 1-9 % was worse than in the previous case, because the fringe spacing was varied, and consequently the average fringe spacing could not be utilized.

When $\boldsymbol{L}$ was in general direction we tried to specify the whole displacement $\boldsymbol{L}$ from single interference pattern, only. Because of small fringes curvature, the angles are not specified with the necessary accuracy, which resulted in a limited determination of $\boldsymbol{L}$. However, this method can be utilized in addition to the method of two or three holograms described by SHIBAYAMA and UCHIYAMA [4].

Les changements simples de l'objet examinè par la méthode d'interférométrie holographique

A l'aide de la méthode d'interférométrie holographique on peut examiner les objets réfléchissants par diffusion et aussi leurs changements complexes. Dans cet article on a considerè les possibilités et la domaine des applications de l'interférométrie holographique à double exposition pour les différents déplacements de l'objet. S'il s'agit des rotations, les conditions de localisation de l'objet doivent être traitées plus soigneusement et c'est purquoi elles sont examinées dans un travail qui suit.

Простые изменения объекта, исследуемого методом голографической интерферометрии

Методом голографической интерферометрии могут исследоваться отражающие диффузионно объекты и их сложные изменения. В статье рассмотрены возможности и область применений голографической интерферометрии с двойной экспозицией для любых смещений объекта. Вращения, при которых трактовка условий локализации объекта должна быть осторожной, составляют предмет очередной работы.

References

[1] STETSON K. A., *Symposium on the Engineering Uses of Holography*, Glasgow, Sept. 1968. Cambridge Press, Cambridge 1970.

[2] FROEHLY C., MONNERET J., PASTEUR J., VIENOT J. Ch. Optica Acta **16** (1969), 343.

[3] TSUJIUCHI J., TAKEYA N., MATSUDA K., Optica Acta **16** (1969), 709.

[4] SHIBAYAMA K., UCHIYAMA H., Applied Optics **10** (1971), 2, 150.

Received, April 17, 1971